

INTERNATIONAL SOCIETY FOR SOIL MECHANICS AND GEOTECHNICAL ENGINEERING



This paper was downloaded from the Online Library of the International Society for Soil Mechanics and Geotechnical Engineering (ISSMGE). The library is available here:

<https://www.issmge.org/publications/online-library>

This is an open-access database that archives thousands of papers published under the Auspices of the ISSMGE and maintained by the Innovation and Development Committee of ISSMGE.

Engineering properties of an expansive soil

Propriétés mécaniques d'un sol gonflant

Azam S., Ito M., Chowdhury R.

Environmental Systems Engineering, University of Regina, Regina, SK, Canada

ABSTRACT: The engineering properties of an expansive soil were investigated using in situ and compacted samples. The soil water characteristic curve was found to have a bimodal shape composing of two air entry values: an initial low value corresponding to macroporous drainage followed by a high value related to microporous flow. Likewise, the shrinkage curve was found to be S-shaped and included a low structural shrinkage followed by a sharp decline during normal shrinkage and then by a low decrease during residual shrinkage.

RÉSUMÉ: Les propriétés mécaniques d'un sol gonflant ont été étudiées à l'aide d'échantillons compactés obtenues sur le terrain. La courbe caractéristique en eau du sol s'est révélé avoir une forme bimodale avec deux valeurs d'entrée d'air: une valeur initiale correspondant à un faible drainage macroporeux suivi d'une valeur élevée par rapport à l'écoulement microporeux. De même, la courbe de rétrécissement est en forme de S et inclus un faible rétrécissement structurelle suivie d'une forte baisse pendant le rétrécissement normal, suivie d'une diminution faible durant le rétrécissement résiduel.

KEYWORDS: expansive soil, soil water characteristic curve, shrinkage curve.

1 INTRODUCTION

The capital of Saskatchewan, Canada, is founded on a glacio-lacustrine clay deposit that exhibits significant volume changes due to seasonal weather variations. Alternate swelling and shrinkage in the expansive Regina clay has impaired civil infrastructure such as transportation networks (Kelly et al. 1995), residential, industrial, and commercial facilities (Ito and Azam 2010), and water supply and sewage collection systems (Hu and Hubble 2005). Damages to engineered facilities are clearly manifested in the form of differential heave in roadways and sidewalks, inclined cracking in slab-on-grade basements and masonry walls, and fatigue and breakage in underground storage tanks and buried pipelines. The associated repair cost is usually quite enormous. For example, the breakage rate in the 850 km long water supply network in the city has now reached a 30-year maximum of 0.27 breaks/km/year, costing more than \$2 million in annual maintenance. Furthermore, the city is currently going through a period of infrastructure development including mega-projects such as the Global Transportation Hub and the Downtown Covered Stadium with a 55000-seat capacity. Clearly, there is a need to study site-specific soil properties for the continuous maintenance and improved design of civil infrastructure systems in Regina.

Generally, volume changes in expansive soils are derived from clay minerals that undergo hydration due to rainfall and dehydration due to evaporation. This process is governed by the attraction of bipolar water molecules to the negatively charged clay particles possessing high specific surface areas (Mitchell and Soga 2005). However, water access to individual clay particles primarily depends on the following two factors: (i) soil structure (micropores within soil peds and macropores between the soil peds) and (ii) soil state (void ratio and degree of saturation). These parameters are respectively governed by parent geology and construction practices prevalent in an area. Recent research on local expansive clays has focused on the determination of unsaturated soil properties using “undisturbed samples” from the geological deposit (Azam and Ito 2011) and

on the correlation of these properties with morphological observations using “cryogenic specimens” in a scanning electron microscope (Ito and Azam 2013). These studies concluded that the geologically-induced soil structure governs the water migration and the swell-shrink patterns through the expansive clay. The present study extends the current body of knowledge to compacted soils thereby capturing the effect of soil state on the the properties of local clays. Overall, a generalized theoretical framework is developed to understand the behavior of expansive soils.

The main objective of this paper is to understand the engineering properties of Regina clay using in situ and compacted specimens. Geotechnical index properties were determined for preliminary soil assessment. The soil water characteristic curve (SWCC) was determined to investigate the water retention capacity of the soil. Likewise, the shrinkage curve was determined to correlate volume changes with soil saturation and desaturation.

2 RESEARCH METHODOLOGY

The expansive clay was retrieved from a local soil deposit that was found to be desiccated in early Fall and exhibited extensive fissuring oriented in all directions. High quality undisturbed samples were obtained using the ASTM Standard Practice for Thin-Walled Tube Sampling of Soils for Geotechnical Purposes (D1587-08) from a depth of 0.6 m to 1.2 m. Likewise, disturbed samples were obtained from bore cuttings according to the ASTM Standard Practice for Soil Investigation and Sampling by Auger Borings (D1452-09). All of the specimens were plastic-wrapped and wax-coated and the entire collection was transported and stored at the University of Regina as per the ASTM Standard Practice for Preserving and Transporting Rock Core Samples (D5079-08). The latter samples were compacted in accordance with the ASTM Standard Test Methods for Laboratory Compaction Characteristics of Soil Using Modified Effort (D1557-12).

The geotechnical index properties were determined according to the ASTM test methods as follows: (i) water content (w) by the Standard Test Methods for Laboratory Determination of Water (Moisture) Content of Soil and Rock by Mass (D2216-05); (ii) dry unit weight (γ_d) by the Standard Test Method for Density of Soil in Place by the Drive-Cylinder Method (D2937-10) for the in situ sample and by the above-mentioned method for the compacted sample; (iii) specific gravity (G_s) by the Standard Test Methods for Specific Gravity of Soil Solids by Water Pycnometer (D854-10); (iv) liquid limit (w_l), plastic limit (w_p) and plasticity index (I_p) by the Standard Test Methods for Liquid Limit, Plastic Limit, and Plasticity Index of Soils (D4318-10); and (v) grain size distribution (GSD) by the Standard Test Method for Particle-Size Analysis of Soils (D422-63(2007)). The entire GSD data is not given in this paper.

The SWCC was determined according to the ASTM Standard Test Methods for Determination of the Soil Water Characteristic Curve for Desorption Using a Hanging Column, Pressure Extractor, Chilled Mirror Hygrometer, and/or Centrifuge (D6836-02(2008)e2) on 10 mm thick samples obtained from both the undisturbed core and the compacted sample. Predetermined values of matric suction were applied using pressure plate and pressure membrane extractors manufactured by Soil Moisture Equipment Inc. These equipment included the following: (i) a 5 bar pressure plate extractor (Model 1600) for up to 200 kPa suction; (ii) a 15 bar pressure plate extractor (Model 1500F1) for suction values ranging from 300 kPa to 500 kPa; and (iii) a 100 bar pressure membrane extractor (Model 1020) for suction values between 2000 kPa and 7000 kPa. The porous plates and the cellulose membranes were submerged in distilled and de-aired water for 24 hours to expel air bubbles. Thereafter, the specimens along with the retaining ring were placed on their respective porous plate or cellulose membrane and allowed to saturate. Next, the excess water was removed and each plate or membrane was placed in the designated extractor. For each suction value, the expelled water from the samples was monitored in a graduated burette. When two consecutive readings nearly matched over a 24 hour period, the test was terminated and the sample water content was determined.

The dew point potentiometer (WP4-T) was used for suction measurement at low water content corresponding to total suction values greater than 7000 kPa. The sampling cup was half filled with soil to ensure accurate suction measurement (Leong et al. 2003) by using about 5 mg of material with a known water quantity. The unsaturated sample was forwarded to the head space of the sealed measurement chamber, set at 25°C temperature, through a sample drawer and was allowed to equilibrate with the surrounding air. Equilibration was usually achieved within 10 min to 20 min, as detected by condensation on a mirror and measured by a photoelectric cell. From knowledge of the universal gas constant, R (8.3145 J/mol^oK), sample temperature, T (°K), water molecular mass, X (18.01 kg/kmol), and the chamber relative humidity, p/p_o , soil suction was calculated ($\psi = RT/X \ln(p/p_o)$) and displayed on the potentiometer screen. The water content of the soil was measured as described earlier.

The shrinkage curve was determined in accordance with the ASTM Standard Test Method for Shrinkage Factors of Soils by the Wax Method (D4943-08). To obtain the void ratio, the volume of soil specimens was determined using the water displacement method. Each specimen was coated with molten microcrystalline wax ($G_s = 0.9$) and allowed to cool down at room temperature. After wax solidification, the sample was submerged in a 250 mL graduated cylinder that was filled with distilled water. The water height in the cylinder was carefully recorded using a Vernier caliper before and after sample submersion in the cylinder. A graduated syringe was used to remove the increased amount of water displaced by the sample

thereby bringing the water height back to the initial reading. The displaced water mass was determined by weighing the graduated syringe before and after water filling and recording the difference. This quantity was readily converted to water volume representing the volume of the wax-coated soil. The volume of soil was obtained from the difference of volume of the wax coated sample and the volume of wax (mass/0.9). A 7.4% correction was applied to account for the underestimation due to air entrapment at the soil-wax interface, as suggested by Prakash et al. (2008). The sample mass was also determined to estimate the bulk unit weight of the soil that, in turn, was converted to the void ratio using basic phase relationships.

3 RESULTS AND DISCUSSION

Table 1 summarizes the geotechnical index properties of the investigated soil. The water content and the dry unit weight of the in situ sample were found to be 31% and 1.34 g/cm³, respectively. In early Fall when the sample was collected, the soil generally experiences a net water deficit given the semi-arid climate prevalent in the region. This was evident from the unsaturated ($S = 82\%$) state of the sample in the field: the field void ratio was calculated to be 1.05. Similar initial conditions ($w = 38\%$ and $\gamma_d = 1.29$ g/cm³) were chosen for the compacted sample to obtain comparable data: the corresponding saturation and void ratio were found to be 86% and 1.18, respectively. The high liquid limit and plastic limit indicate the high water adsorption capability of the clay. These values are attributed to the presence of expansive clay minerals such as smectite, hydrous mica, and chlorite (Ito and Azam 2009). Likewise, the clay size fraction (material finer than 0.002 mm) was found to be around 65%. The fine grained nature of the soil suggests a high water retention capacity. The calculated soil activity ($A = I_p / C$) of about 0.8 is associated with moderate swelling. Overall, the soil was classified as CH (clay with high plasticity) according to the Unified Soil Classification System (USCS).

Table 1. Summary of geotechnical index properties

Property	In situ	Compacted
Water Content, w (%)	31	38
Dry Unit Weight, γ_d (g/cm ³)	1.34	1.29
Specific Gravity, G_s	2.75	2.74
Void Ratio, e^*	1.05	1.18
Degree of Saturation, S (%)†	81	86
Liquid Limit, w_l (%)	83	77
Plastic Limit, w_p (%)	30	27
Plasticity Index, I_p (%)	53	50
Clay Size Fraction, C (%)	66	64
USCS Symbol	CH	CH

$$* e = (G_s \gamma_w / \gamma_d) - 1$$

$$† S = w G_s / e$$

Figures 1 shows SWCC with gravimetric water content. The samples were put in a water tub for one week and the water content measured 38% for the in situ sample and 46% for the compacted sample. Irrespective of the initial water content, the SWCC data fitted well to bimodal distributions with two air entry values: a lower value (10 kPa) corresponding to drainage through fissures followed by a higher value (300 kPa and 100 kPa for the two samples, respectively) associated with seepage through the soil matrix. When the samples were gradually desaturated, air first entered into the fissures at low suction.

Although the fissures are sealed due to hydration of clay minerals, these discontinuities have much lower tensile strengths than the soil aggregates (Azam and Wilson 2006). This led to a quick drainage through these paths of least resistance. Subsequent application of suction affected the soil aggregates and eventually forced air to enter into the pore system of the aggregate. The upward SWCC shift of the compacted sample with respect to the in situ sample is attributed to the high initial water content of the former sample. Upon water inundation, this sample favored particle hydration because of a comparatively looser state ($e = 1.18$). Likewise, the relatively homogeneous structure of the compacted sample correlated well with its smaller difference between the two air entry values. The effect of soil structure was eliminated when the two curves merged at higher suction. Desaturation occurred at an increased rate up to residual suction of 200000 kPa ($w = 5\%$) and the curves finally joined the abscissa at 10^6 kPa.

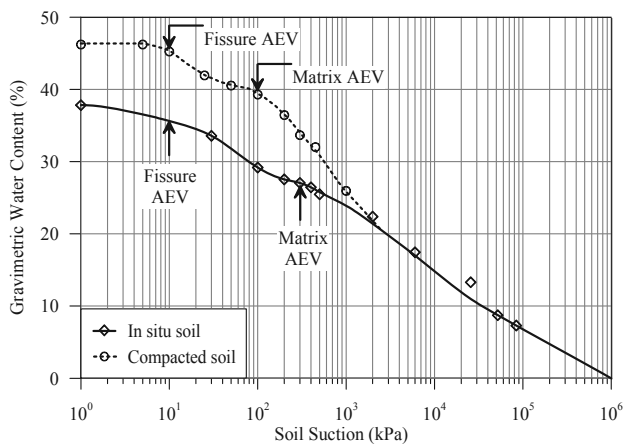


Figure 1. SWCC with gravimetric water content

Figure 2 presents the SWCC in the form of void ratio as a function of soil suction. The measured data closely followed unimodal distributions showing a single air entry value (300 kPa for the in situ sample and 100 kPa for the compacted sample). The latter sample plotted at a higher void ratio at low suction and merged with the in situ sample at 500 kPa. Thereafter, the singular curve exhibited a sharp decrease in void ratio up to the residual condition, became asymptotic to the abscissa after the residual suction and never reporting to 10^6 kPa on complete drying. This is because void ratio of a soil pertains to an average value for all voids and does not differentiate between inter-aggregate fissures and intra-aggregate pores. Clearly, SWCC representation in the form of void ratio is not suitable for expansive soils.

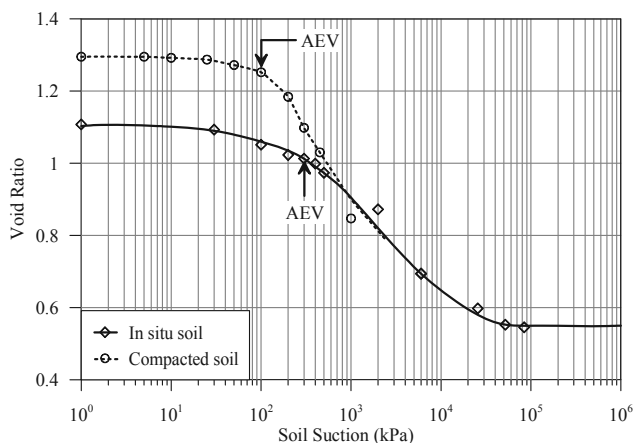


Figure 2. SWCC with void ratio

Figure 3 gives the SWCC in the form of degree of saturation versus suction. Similar to Figure 1, the laboratory measured

data depicted a bimodal function with a fissure air entry value of 10 kPa. For the in situ sample, the average degree of saturation decreased due to drainage through fissures and reached about 70% when most of the fissures were filled with air. The corresponding saturation for the compacted sample was found to be around 85% indicating the presence of relatively smaller and less frequent discontinuities. Once the fissures were desaturated, water flow had to occur through voids in the soil aggregates. Microporous drainage required a high suction (6000 kPa) for air to enter into the soil matrix. In contrast to Figure 1, the significantly higher matrix air entry value in this figure is attributed to the gradual decrease in soil volume with increasing suction. As explained later, this volume reduction is primarily due to reduced fissure sizes and, as such, was not captured in Figure 2 that is based on an average void ratio.

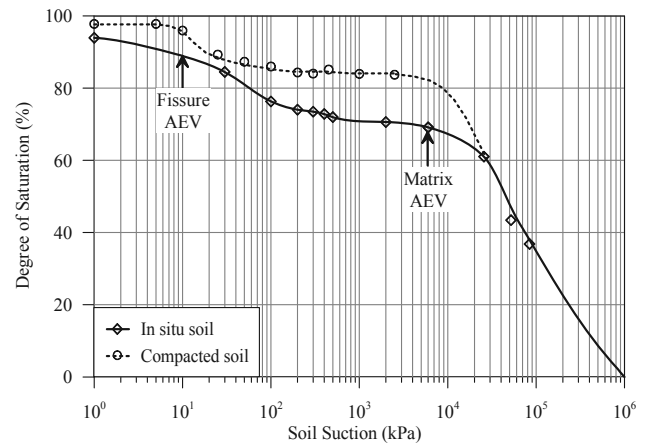


Figure 3. SWCC with degree of saturation

The SWCC given in the form of water content versus matric suction is the most accurate representation for expansive soils. This is because gravimetric water content (measured for each suction value) captures the water drainage through fissures and is independent of volume changes due to water adsorption by clay particles. Likewise, the SWCC represented in the form of degree of saturation versus soil suction is most suitable for understanding volume decrease in fissures due to suction application. Marinho (2005) reported that for plastic soils, drainage through water filled pores is associated with pore compressibility due to capillarity and this phenomenon renders such soils to remain saturated over higher suction values. This representation implies that the expansive soil aggregates remain saturated over a wider range of suction generally prevalent in the field, as postulated by Fityus and Buzzi (2008).

Figure 4 shows the shrinkage curve for the investigated expansive clay. Theoretical lines representing various average saturation degrees were obtained from basic phase relationships and using $G_s = 2.75$. The initially unsaturated samples were first wetted to achieve close to saturation conditions and subsequently desaturated by applying different suction values. The void ratio and water content of each sample were determined as described earlier in this paper. The data depicted in Figure 4 indicate S-shaped shrinkage curves for both sample types and represent the progressive drying of the investigated expansive soil. The curves are composed of an initial low structural shrinkage followed by a sharp decline during normal shrinkage and then by a low decrease during residual shrinkage (Haines, 1923). During structural shrinkage, water within the fissures and some of the larger and relatively stable voids is removed such that the decrease in soil volume is less than the volume of water lost. Volume decrease in soil is equal to the volume of water lost during normal shrinkage thereby leading to a 45° straight line, which is almost parallel to the 100% saturation line. This suggests that drainage primarily takes place through the soil matrix in the normal shrinkage zone. During

residual shrinkage, air enters the pores close to the shrinkage limit and pulls the particles together due to suction. This leads to a further decrease in soil volume albeit lower than the volume of water lost. Furthermore, the high volume change and the closeness to the saturation line during normal shrinkage corresponded well with the comparatively looser state and a relatively homogeneous structure of the compacted sample. Finally, the observed shrinkage curve is reversible because the in situ soil has undergone numerous swell-shrink cycles since deposition. Likewise, Tripathy et al. (2002) reported that equilibrium conditions are usually attained after about four cycles in compacted soils.

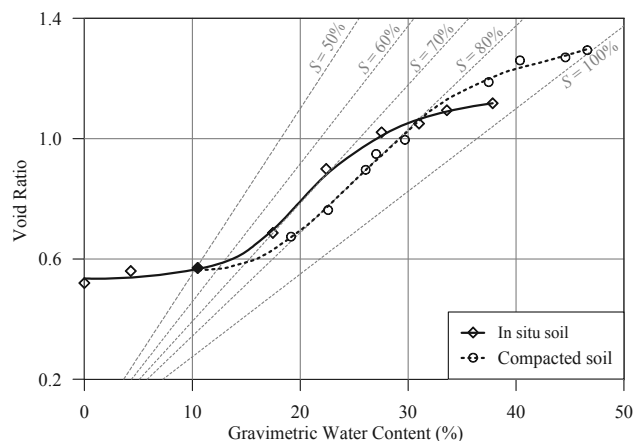


Figure 4. Shrinkage curve

Theoretically, the shrinkage curve comprises of two straight lines: a sloped line closely following the $S = 100\%$ line that joins a horizontal line at a void ratio associated with the shrinkage limit of the soil. This means that soils essentially remain saturated up to the shrinkage limit following a J-shaped curve. Due to the presence of fissures, the investigated soil (in both in situ and compacted conditions) exhibited deviations from this theoretical behavior.

The definition the degree of saturation for expansive soils is not straight forward. Since such soils consist of discontinuities and soil aggregates, the calculated degree of saturation pertains to an average value for the entire soil mass. This definition was used in Figure 3 because it permits easy calculations. A more accurate approach is to consider only the soil aggregates as saturated up to the matrix air entry value of Figure 3 and the fissures as air filled cracks. This is close to an equilibrium soil microstructure that allows alternate swelling and shrinkage. In this approach, the change of water volume in the soil mass equates to the volume change of the soil aggregates and that of the cracks. Gens and Alonso (1992) explained the two levels of soil structure in their framework as follows: the micro-level is governed by physicochemical interactions between the expansive clay minerals thereby forming aggregates whereas the macro-level includes both the aggregates and the fissures.

Overall, water flow through expansive soils is governed by soil structure as indicated by bimodal SWCCs for both undisturbed and compacted samples: sample type becomes irrelevant when the flow starts to occur through the soil matrix. Likewise, the S-shaped swell-shrink curve confirms the structure dominant volume change behavior of such soils for both samples. In the absence of an adequate definition for the degree of saturation, soil state pertains to the initial void ratio. This parameter governs the extent of volume change that, in turn, must be calculated from the reversible swell-shrink curve for expansive soils.

4 CONCLUSIONS

The engineering properties of a typical expansive soil (from Regina, Saskatchewan, Canada) were investigated under in situ and compacted conditions. For both sample types, the clay behavior was characterized by its internal structure comprising of fissures and aggregates. The SWCC using water content on the ordinate showed a bimodal distribution with two air entry values: a lower value (10 kPa) corresponding to drainage through fissures followed by a higher value (300 kPa) for the in situ sample and 100 kPa for the compacted sample) associated with seepage through the soil matrix. Sample type became irrelevant when the flow started to occur through the soil matrix. The matrix air entry value was found to be about 6000 kPa when the SWCC was plotted in the form of the degree of saturation versus soil suction. Likewise, the shrinkage curve was found to be S-shaped and included a low structural shrinkage followed by a sharp decline during normal shrinkage and then by a low decrease during residual shrinkage. The extent of volume change that depends on the initial void ratio must be calculated from the reversible swell-shrink curve.

5 ACKNOWLEDGEMENTS

The authors acknowledge the material and financial support provided by the Saskatchewan Ministry of Highways and Infrastructure and the University of Regina for providing laboratory space.

6 REFERENCES

- Azam S. and Ito, M. 2011. Unsaturated soil properties of a fissured expansive clay. *Proceedings, 64th Canadian Geotechnical Conference*, Toronto, Canada. 313:1-5.
- Azam, S. and Wilson, G.W. 2006. Volume change behavior of a fissured expansive clay containing anhydrous calcium sulfate. *Proceedings, 4th International Conference on Unsaturated Soils*, Carefree, Arizona, USA. 1, 906-915.
- Fityus, S. and Buzzi, O. 2008. The place of expansive soils in the frameworks of unsaturated soil mechanics. *Applied Clay Science* 43, 150-155.
- Gens, A. and Alonso, E.E. 1992. A framework for the behaviour of unsaturated expansive clays. *Canadian Geotechnical Journal* 29, 1013-1032.
- Haines, W.B. 1923. The volume change associated with variations of water content in soil. *Journal of Agricultural Science* 13, 296-310.
- Hu, Y. and Hubble, D.W. 2005. Failure conditions of asbestos cement water mains. *Canadian Geotechnical Journal* 34, 608-621.
- Ito, M. and Azam, S. 2013. Engineering properties of a vertisolic expansive soil deposit. *Engineering Geology*. 152(1):10-16
- Ito, M. and Azam, S. 2010. Determination of swelling and shrinkage properties of undisturbed expansive soils. *Geotechnical and Geological Engineering* 28, 413-422.
- Ito, M. and Azam, S. 2009. Engineering characteristics of a glacio-lacustrine clay deposit in a semi-arid climate. *Bulletin of Engineering Geology and the Environment* 68, 551-557.
- Kelly, A.J., Sauer, E.K., Barbour, S.L., Christiansen, E.A., and Widger, R.A. 1995. Deformation of the Deer Creek bridge by an active landslide in clay shale. *Canadian Geotechnical Journal* 32, 701-724.
- Leong, E.C., Tripathy, S. and Rahardjo, H. 2003. Total suction measurement of unsaturated soils with a device using the chilled-mirror dew-point technique. *Geotechnique* 53, 173-182.
- Marinho, F.M.A. 2005. Nature of soil-water characteristic curve for plastic soils. *Journal of Geotechnical and Geoenvironmental Engineering* 131, 654-661.
- Mitchell, J.K. and Soga, K. (2005). *Fundamentals of Soil Behaviour*. 3rd ed., John Wiley and Sons, Inc. New York, NY, USA.
- Prakash, K., Shidharan, A. Baba, J.A., and Thejas, H.K. 2008. Determination of shrinkage limit of fine-grained soils by wax method. *Geotechnical Testing Journal* 32, 86-89.
- Tripathy, S., Subba Rao, K.S., and Fredlund, D.G. 2002. Water content-void ratio swell-shrink paths of compacted expansive soils. *Canadian Geotechnical Journal* 39, 938-959.